Correlation of texture and intergranular corrosion in Al-Mg 5xxx series alloys

O Engler, T Hentschel and H-J Brinkman
Hydro Aluminium Rolled Products, R&D Bonn, PO Box 2468, D-53014 Bonn, Germany
E-mail: olaf.engler@hydro.com

Abstract. Aluminium-alloys of the AA 5xxx series with Mg contents in excess of 3% may suffer from intergranular corrosion (IGC) when exposed to temperatures in the range 60 to 200°C. At these temperatures Al-Mg alloys are rendered susceptible to IGC by precipitation of β-Al_8Mg_5 phases along the grain boundaries. Accordingly, susceptibility to IGC will depend on grain size as well as type and orientation of the grain boundaries present in the material, that is, on the crystallographic texture of the material at final gauge.
Therefore, it is of great interest to study the correlation of texture and precipitation of β-AlMg phases and, therewith, susceptibility to IGC. For this purpose, different AA 5182 samples were processed so as to produce different crystallographic textures and characterized with respect to microstructure and resistance against IGC. EBSD local texture analysis was applied to provide information about the grain boundary character distribution. Eventually, this may enable Al industry to reduce the susceptibility of Al-Mg alloys to IGC by proper control of the final gauge texture, such that higher Mg-contents may be used in IGC-critical applications.

1. Introduction

Aluminium alloys of the AA 5xxx series with Mg contents in excess of 3% may suffer from intergranular corrosion (IGC) when they are exposed for a long time to temperatures in the range 60 to 200°C [1,2]. At these temperatures Al-Mg alloys are rendered susceptible to IGC by precipitation of β-Al_8Mg_5 phases along the grain boundaries. Fig. 1(a) shows an example of alloy AA 5182 with about 4.5% Mg, which was heat treated for 17 h at 130°C. The sample was etched for 30 min in 6% phosphoric acid (BSI-test) so as to reveal the spatial arrangement of β-Al_8Mg_5 phase particles. Obviously, in this heavily sensitized condition the β-Al_8Mg_5 particles have precipitated along the grain boundaries which, in the presence of a corrosive medium, renders the material susceptible to IGC (Fig. 1(b)). For these reasons, 5xxx alloys for IGC-critical automotive applications are generally limited to Mg-contents below 3%, which prevents industry from utilizing the full strength potential and, in turn, the full potential for weight savings of 5xxx series alloys.
Volume and rate of precipitation of β-Al_8Mg_5 phases along the grain boundaries will depend on density, type and orientation of the grain boundaries present in the material, that is, on the grain size and on the crystallographic texture of the material at final gauge. Regarding texture, it has recently been demonstrated that there is a clear correlation between texture and resistance against IGC in 5xxx series alloys [3]. For two differently processed samples of alloy AA 5182 a decrease in IGC mass losses from 40 mg/cm² down to 30 mg/cm² could unequivocally be ascribed to different texture, more specifically, to differences in the grain boundary character distribution of the two sheets. More specifically, a batch-annealed sample with a weak cube recrystallization texture plus retained rolling texture had better IGC stability than a flash annealed sample with a more pronounced cube texture. The texture of the batch annealed had a higher density of special CSL-grain boundaries and, most notably, low-angle grain boundaries which are known to play a key role in the resistance to IGC [4,5].
In the present study we have applied the above information on correlation of texture and IGC so as to improve the corrosion behaviour of alloy AA 5182. For this purpose AA 5182 hot strips were taken from two different hot mills, which are known to produce different hot strip texture. Then, the hot strips were lab-processed with and without inter-annealing to final gauge in order to explore the texture differences that can be produced in an industrial setting. The materials were characterized with respect to microstructure, texture and resistance against IGC. Eventually, this may enable us to reduce the susceptibility of Al-Mg alloys to IGC by proper control of the final gauge texture, such that higher Mg-contents may be used for IGC-critical applications.

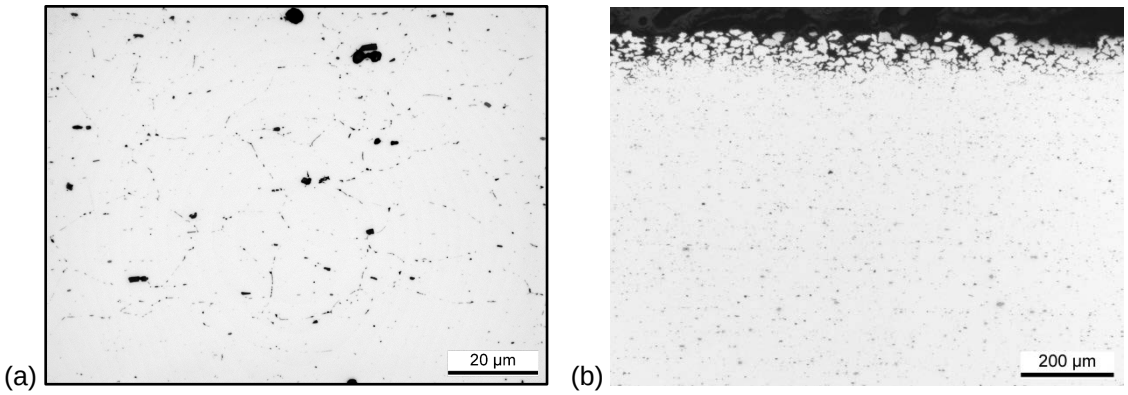

Fig. 1. Micrographs of AA 5182 after sensitization annealing for 17 h at 130°C. (a) BSI-etched, showing grain boundary precipitation; (b) microstructure after NAMLT test, showing heavy corrosion attack by IGC (longitudinal section).

2. Experimental

In the present study two hot strip samples of AA 5182 (EN AW-5182 / ISO: Al Mg4.5 Mn0.4) were sourced from different hot mills. Both samples, referred to as I and II, revealed a fine grained, fully recrystallized microstructure, but were differentiated by their recrystallization texture. Samples from the two hot strips were processed on the lab facilities of the Hydro R&D Center in Bonn so as to ensure maximum comparability of the down-stream processing. One set of samples was cold rolled by a total thickness reduction of 50% and soft annealed with a simulated batch annealing practice (peak temperature 350°C) with a controlled cooling cycle. The second set of samples was cold rolled 50%, inter-annealed, again rolled 50% and then soft annealed as described before. The third series of samples was cold rolled in several passes to a total of 75% without inter-annealing, before being soft annealed.

Susceptibility to IGC was determined in the standard nitric acid mass loss test (NAMLT) according to ASTM G67. Samples were tested both in the as-received condition (“none”) and following an artificial sensitization treatment for 17 h at 130°C. For each material and state two specimens with a size of approximately 50 × 60 mm² were prepared and the weight loss was determined after submersion of the samples in concentrated nitric acid for 24 h.

Grain size was determined by quantitative image analysis in optical micrographs, obtained by anodical oxidation in longitudinal sections of the sheet samples. Crystallographic textures of the sheets were determined at about quarter thickness by standard X-ray diffraction techniques at RWTH Aachen [6]. From several pole figures the 3-dimensional orientation distribution functions (ODFs) *f(g)* were calculated by the series expansion method [7]. The ODFs were corrected with respect to the so-called ghost error following the positivity method of Dahms and Bunge [8] and represented by plotting iso-intensity lines in three characteristic sections with φ_2 =45°, 65° and 90° through the Euler orientation space. Preliminary EBSD analysis performed close to the sheet surface proved that the textures of the sub-surface layers were quite similar as the bulk textures, which is characteristic of a homogeneous plane-strain state upon cold rolling of thin sheet.

3. Results

It is known that the susceptibility to IGC depends on grain size, with small grain size being more prone to IGC than larger grains. Therefore, for all samples the grain sizes were determined quantitatively; two examples with noticeably different grain sizes are presented in Fig. 2. The hot strip samples showed some variation in average grain size, viz. 15 µm (I) and 19 µm (II), respectively. After cold rolling and soft annealing the differences between the two variants largely vanished, however. For the samples with a rolling degree of 50% the final grain size varied between 15 and 17 µm (e.g. Fig. 2(a)); two passes of 50% with inter-annealing led to very similar results. After two consecutive 50% passes without inter-annealing (i.e. a total of 75%) the final grain size was smaller, some 11-12 µm (Fig. 2(b)), but again there were no differences among the two different hot strip variants.

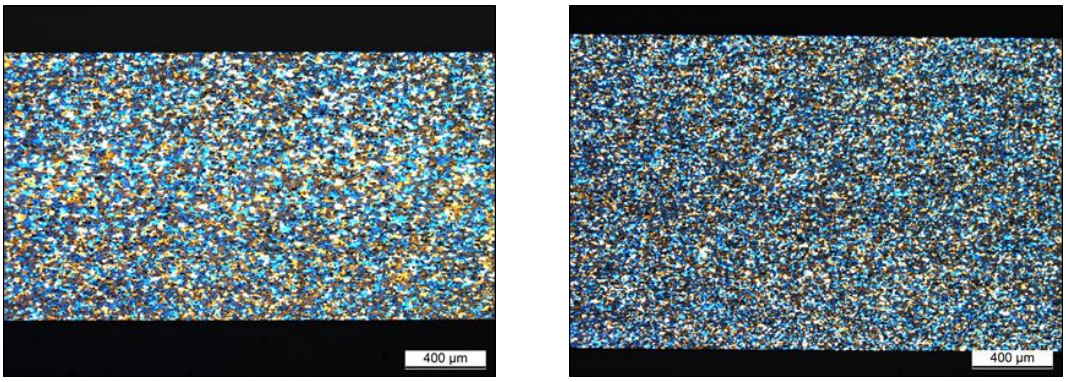

(a) I – 50% rolled (b) II – 75% rolled

Fig. 2. Microstructure of two specimens with different grain size
(a) hot strip I – 50% cold rolled, (b) hot strip II – 75% cold rolled.

Fig. 3 summarizes the results from the NAMLT test in terms of the IGC mass losses for the various samples. It appears that in all cases the additional heat treatment of 17 h at 130°C significantly amplified the mass losses, yet without changing the relative ratio between different samples. For the hot strip I (labelled "0%" in Fig. 3) mass losses were larger than for hot strip II. This tendency exactly followed the grain size data of the two hot strips.

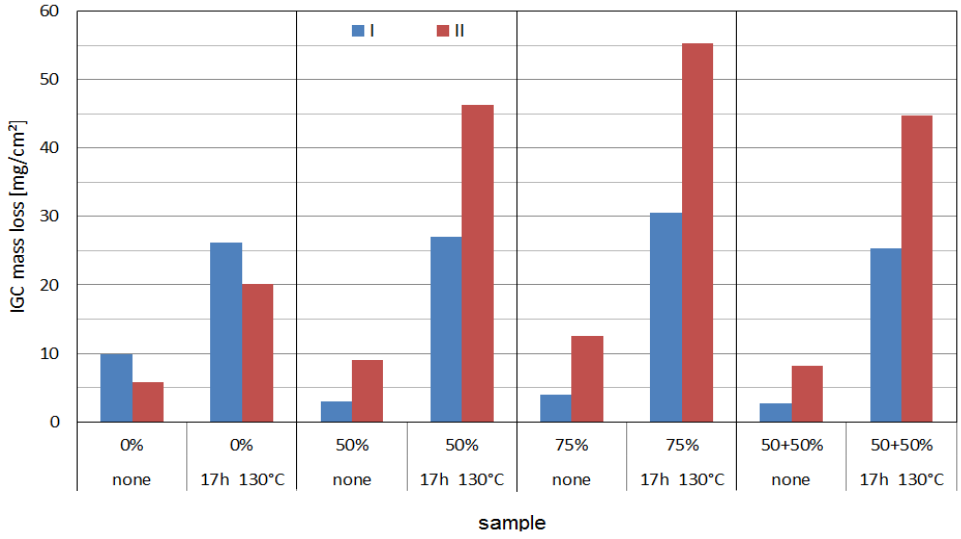

Fig. 3. IGC mass losses during NAMLT testing for the various samples.

After down-stream processing these findings were reversed, however. In all cases material II revealed larger mass losses than material I. With a view to the three different processing routes it turned out that the 75% cold rolled samples had highest mass losses. 75% cold rolling with inter-annealing (i.e. 50% + 50%) or a single pass of 50% both gave noticeably better resistance to IGC, in contrast (Fig. 3). These differences are again ascribed to the significantly lower grain size in the 75% rolled material (Fig. 2). Note that both the quantitative mass loss data and, especially, the differences between the differently processed sheets are comparable to the results obtained in the previous study [3].
Results of the texture measurements are presented in Figs. 4 – 7 in the form of the ODFs obtained for the various hot strips and the three different processing routes, respectively. As already alluded to earlier, the textures are all comprised of the cube recrystallization texture as well as orientations of the retained rolling texture with varying ratios. Hot strip I had a quite sharp cube texture with a maximum intensity $f(g)$ = 18 together with some retained rolling texture (Fig. 4(a)). Such textures which are characteristic of multi-pass tandem lines are typically encountered in AA 3104 can body stock (e.g. [9]).

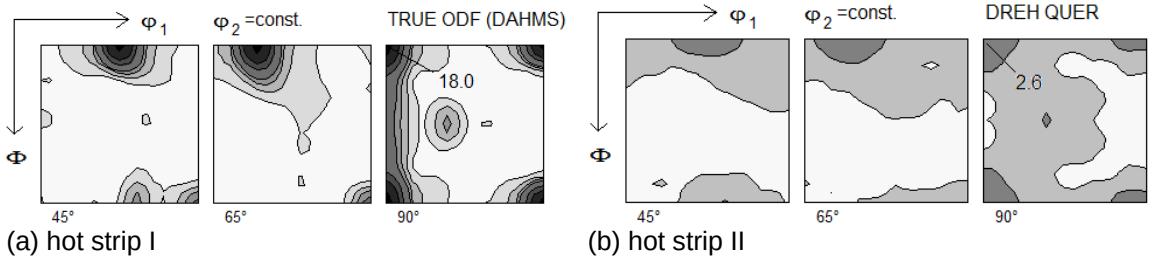

Fig. 4. ODFs of the two different hot strip samples.

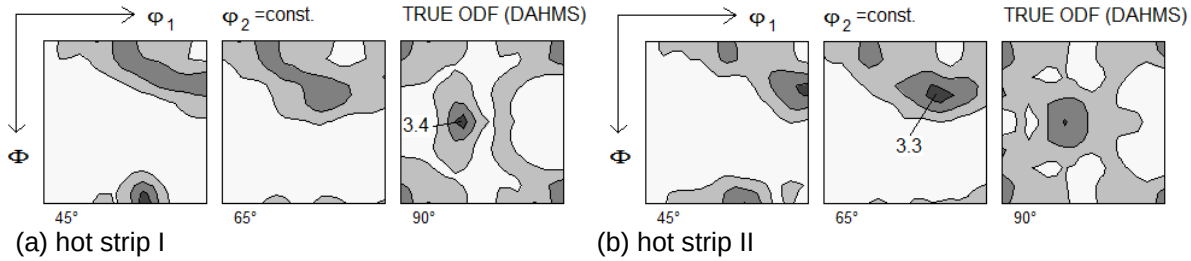

Fig. 5. ODFs of the two hot strips after 50% cold rolling and recrystallization.

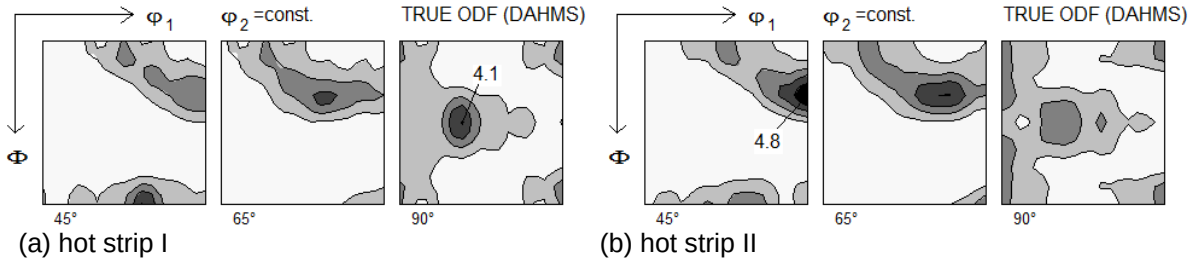

Fig. 6. ODFs of the two hot strips after 75% cold rolling and recrystallization.

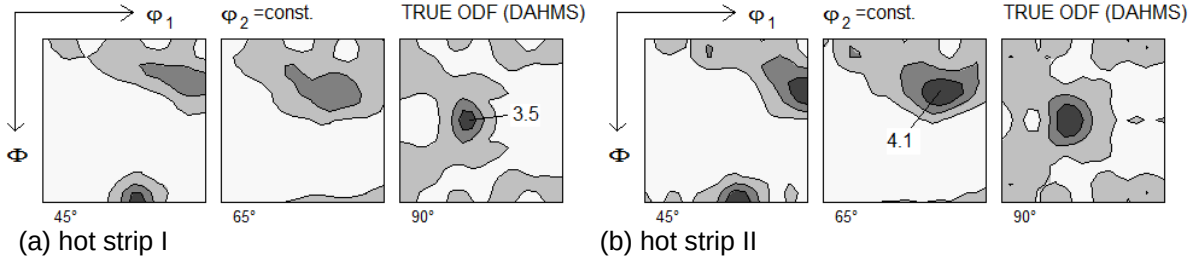

Fig. 7. ODFs of the two hot strips after 75% cold rolling with inter-annealing (50%+50%).

All other textures – hot strip II as well as all cold rolled and soft annealed samples – were quite weak, with maximum intensities ranging from 3 to 5. The texture results of the 75% rolled samples are further summarized in Fig. 8 in form of their main texture fibres, viz. (i) the cube$_{RD}$-fibre comprising the cube-orientation with its RD-scatter (open symbols) and (ii) the β-fibre with the retained rolling texture orientations (filled symbols). Evidently, in both variants the intensities of the retained rolling texture orientations notably exceed those of the cube$_{RD}$-fibre. It is noted that in all cases the samples of series I revealed lower intensities, for both the cube$_{RD}$-fibre and, especially, the retained rolling texture orientations (Figs. 5 – 8).

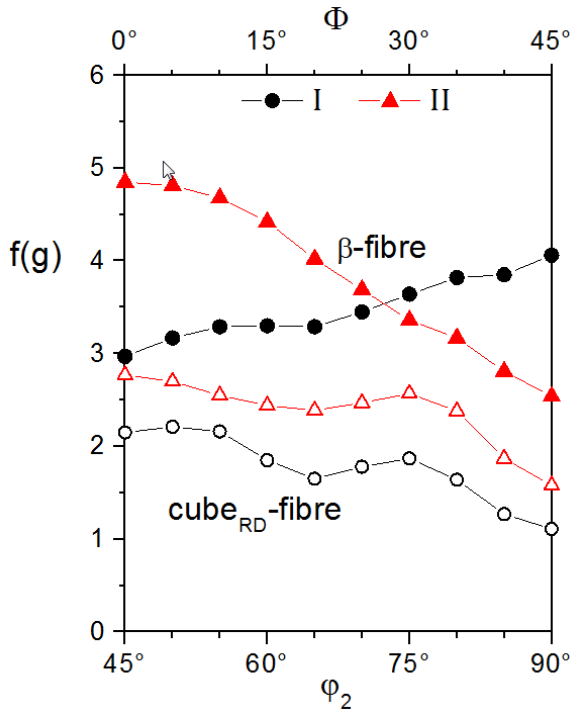

Fig. 8. Texture intensities along the cube$_{RD}$-fibre (open symbols) and β-fibre (filled symbols) for the two 75% rolled samples.

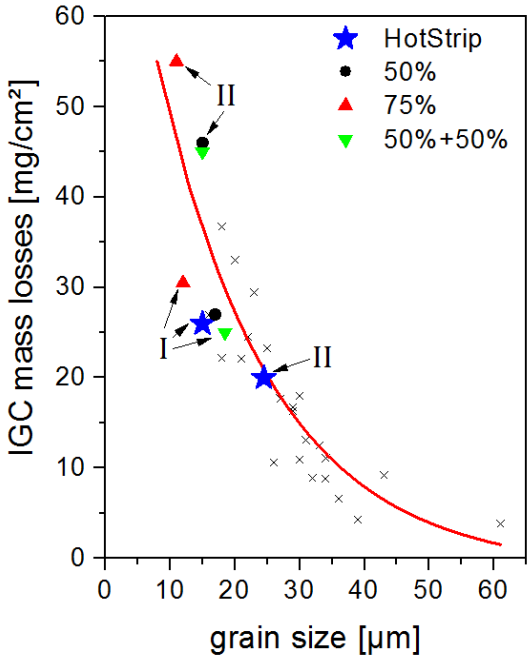

Fig. 9. Mass losses due to IGC in alloy AA 5182 as a function of grain size (sensitized for 17 h at 130°C).

Within the individual series I and II it appears that the 75% rolled sample revealed strongest β-fibre intensities, followed by 50%+50% and, finally, 50%. For the cube$_{RD}$-fibre orientations the sequence is slightly different: 75% is again strongest, but followed by 50% and then 50%+50% (Figs. 5 – 7).
It is worthwhile emphasizing that in all cases the texture evolution followed the well-known patterns of texture formation during cold rolling and recrystallization in Al alloys, see, e.g., Refs. [9-11].

4. Discussion and conclusions

As already stated above, intergranular corrosion (IGC) in Al-Mg alloys depends on grain size and on the crystallographic texture of the material at final gauge. Fig. 9 shows a plot of the mass losses due to IGC in alloy AA 5182 as a function of grain size, revealing an appreciable reduction in mass losses with increasing grain size. Comparison of the dependency on grain size summarized in Fig. 9 with the different mass losses obtained in the previous study [3] suggests that the influence of grain size is much bigger than that of texture. Accordingly, the differences in IGC mass losses of the two different hot strip samples can readily be attributed to the different grain sizes of the same, while a possible impact of texture may be screened.
In order to study this more deeply, Fig. 9 also contains the IGC data for the two hot strips, revealing that the results for hot strip II come to lie rather close to the red best-fit curve. Sample I shows slightly lower mass losses than what would be expected for the actual grain size, however, which, with all due care, seems to imply that the actual texture is beneficial in improving IGC resistance in this very material. This material I with its pronounced cube recrystallization texture (Fig. 4(a)) will comprise a rather high fraction of low-angle grain boundaries, whereas hot strip II with a very weak hot strip texture (Fig. 4(b)) will presumably comprise a much higher fraction of high-angle grain boundaries, similar to the well-known Mackenzie-distribution for randomly oriented microstructures [6]. Low-angle boundaries are

known to play a key role in the resistance to IGC, in that these boundaries were previously found to be most resistant to corrosion in high-purity Al [4].
After down-stream processing (cold rolling and soft annealing) it was observed that the 75% cold rolled samples had higher mass losses than the 50% cold rolled samples (both one pass or two passes with inter-annealing, i.e. 50%+50%; Fig. 3). Again, these differences can readily be attributed to the significantly lower grain size in the 75% rolled material (Fig. 2).
Vice versa, a direct impact of texture on IGC can only be derived for samples with identical grain size. In the present study this applies to the three series with identical down-stream processing, i.e. 50°, 50%+50% and 75%, respectively. Within these three processing routes it turned out that alloy II always revealed higher mass losses due to IGC than material I (Fig. 3). The IGC results are also marked in Fig. 8, indicating that despite some subtle differences in grain size the mass losses of material II tend to lie closer to the red best-fit curve than those of material I.
Thus, it may be concluded that the weak mixed textures composed of the cube recrystallization texture and some retained rolling texture orientations (e.g. Figs. 5 – 7) reveal optimum conditions for exhibiting resistance against IGC. The reason for the differences between the current materials I and II with rather similar mixed textures could not be clarified yet, however. In the previous study it was shown that preferable textures were characterized by a high density of 'special' CSL-grain boundaries and, most notably, low-angle grain boundaries [3]. Both low-angle grain boundaries and special CSL-boundaries are commonly assumed to have lower energy than regular high-angle grain boundaries (e.g. [12]). As precipitation of β-Al_8Mg_5 phases preferably occurs along un-ordered high-energy boundaries, an increased fraction of special boundaries will reduce precipitate formation, thus reducing IGC intensity [4,5]. A detailed classification of the grain boundary character distribution of the two materials is currently being performed by means of EBSD local texture analysis.

References

[1] Searles JL, Gouma PI and Buchheit RG 2001 *Metall. Mater. Trans.* **32A** 2859-2867
[2] Tan L and Allen TR 2010 *Corrosion Sci.* **52** 548-554
[3] Hill L, Randle V and Engler O 2013 *Mater. Sci. Tech.* **29** 1006-1011
[4] Kim SH, Erb U, Aust KT and Palumbo G 2001 *Scripta Mater.* **44** 835-839
[5] Aust KT, Erb U and Palumbo G 1994 *Mater. Sci. Eng.* **A176** 329-334
[6] Engler O and Randle V 2010 *Introduction to Texture Analysis: Macrotexture, Microtexture and Orientation Mapping* (Boca Raton, FL: CRC Press)
[7] Bunge HJ 1982 *Texture Analysis in Materials Science* (London: Butterworths)
[8] Dahms M and Bunge 1989 *J. Appl. Cryst.* **22** 439-447
[9] Engler O, Löchte L and Hirsch J 2007 *Acta Mater.* **55** 5449-5463
[10] Engler O, Crumbach M and Li S 2005 *Acta Mater.* **53** 2241-2257
[11] Engler O and Hirsch J 2009 *Inter. J. Mater. Res.* **100** 564-575
[12] Lin H and Pope DP 1995 *Mater. Sci. Eng.* **A394** 192-193